

## LASERS AND THEIR APPLICATION

# Increasing Pumping Efficiency by Using Gradient-Doped Laser Crystals

E. V. Stroganova, V. V. Galutskiy, D. S. Tkachev, N. N. Nalbantov,  
A. A. Tsema, and N. A. Yakovenko

Kuban State University, Krasnodar, 350040 Russia

e-mail: stroganova@phys.kubsu.ru

Received August 23, 2013; in final form, July 13, 2014

**Abstract**—Investigations of a new class of optical materials with functional nonuniform distribution of optical dopant are continued. Longitudinal pumping and heat release in active elements with a gradient distribution of optical centers are simulated. It is shown that, for a given length of the laser element, pumping efficiency remains at a stably high level upon variation of its power density for different gradients of concentration of activators. It is demonstrated that, in addition to a high level of optical pumping efficiency, the temperature profile in the active medium becomes smoother.

**DOI:** 10.1134/S0030400X14120236

## INTRODUCTION

When new high-efficiency lasers are developed, special attention is paid to their threshold intensity and the limiting pump power of laser elements (LEs). On the one hand, a low threshold allows achieving a high pumping efficiency of active elements. On the other hand, high pump power induces thermal effects in laser elements in the form of thermal lenses, which lowers the laser efficiency. Methods of increasing efficiency of the diode-pumped lasers by changing the active element geometry at a constant doping level or the shape of the pump pulse were proposed in [1–3]. The main goal in these methods is achieving maximum possible pump efficiency, i.e., the maximum ratio of the number of emitted photons to the number of pump photons absorbed in the laser element within the pump pulse. There are other ways to increase the efficiency of longitudinal pumping of lasers. One of them consists in using a new class of optical materials—namely, crystals with nonuniform distribution of doping impurity along the growth direction [4, 5], for fabrication of laser elements. Such technologies [4] allow creating an arbitrary distribution of optical dopant concentration along the active element. In the present work, we analyze some such experimentally realized and grown crystals exhibiting a gradient of optical dopant concentration [4, 5] from the point of view of their influence on longitudinal pumping efficiency.

## METHODS

Monocrystals with a specified gradient of optical impurity concentration (YAG:Nd, YAG:Yb, LiNbO<sub>3</sub>:Yb, LiNbO<sub>3</sub>:Er, LiNbO<sub>3</sub>:Yb,Er) were synthe-

sized and grown for the first time at Kuban State University [4] by using the Czochralski method with continuous liquid replenishment. Concentration profiles of the grown crystals are presented in Fig. 1. The correlation between the theoretical concentration profile and the actual gradient of concentration of optical centers was determined by means of spectral-kinetic studies described in [5]. To determine the longitudinal

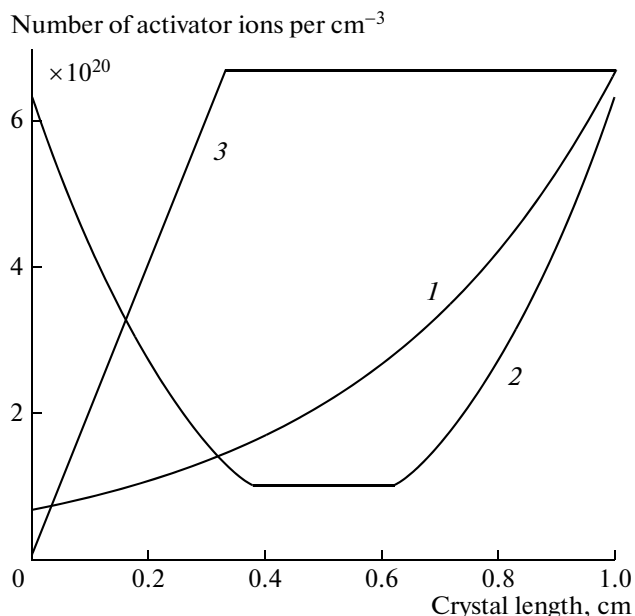


**Fig. 1.** Profiles of Yb<sup>3+</sup> concentration in YAG crystal: (1) exponential, (2) parabolic, and (3) linearly increasing, leveling off.

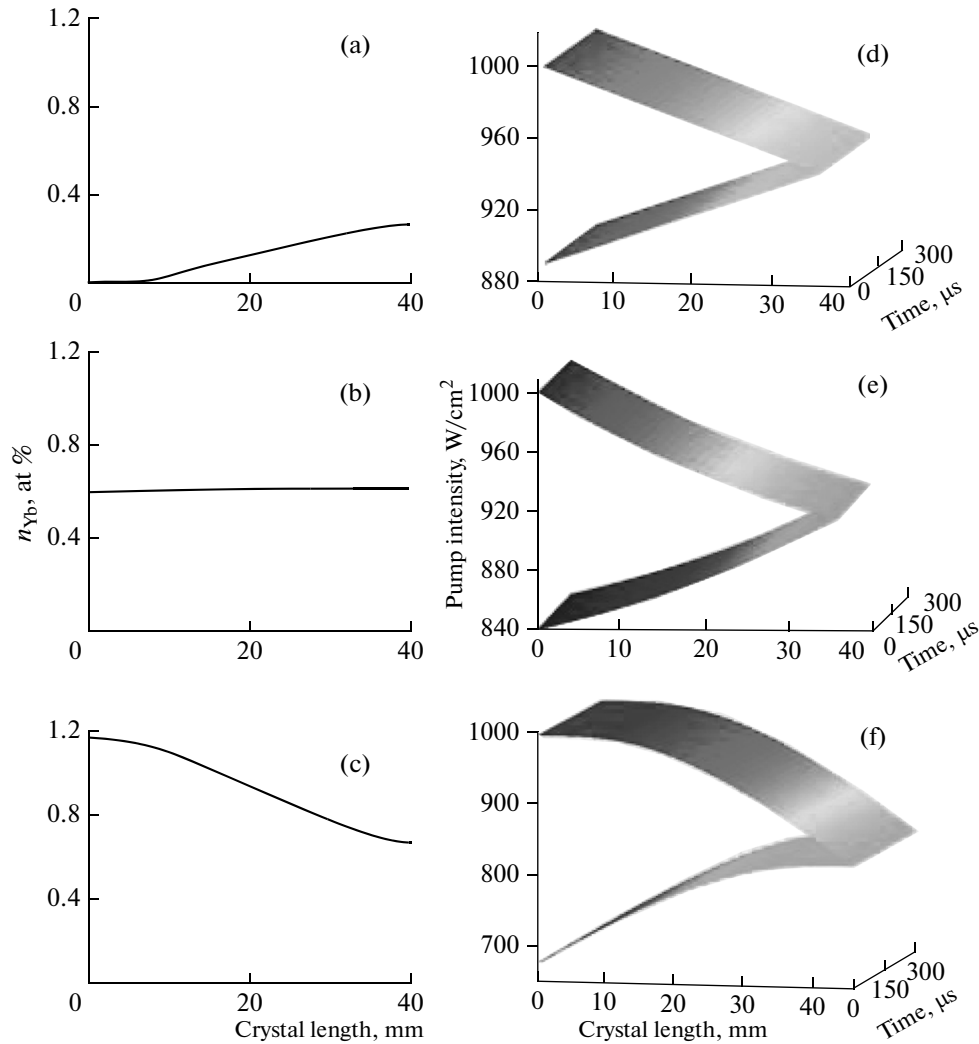


**Fig. 2.** Distribution of absorbed pump energy for incident and reflected waves in a laser element (d–f) for different profiles of concentration of optical centers (a–c), respectively.

pumping efficiency of the laser element, we used a physical model [2] of pump power distribution,

$$\begin{aligned} \frac{\partial I^{(+)}(z, t)}{\partial z} &= -(+) \sigma (f_a N_0(z, t) - f_b N_1(z, t)) I^{(+)}(z, t), \\ \frac{\partial N_1(z, t)}{\partial t} &= \sigma (f_a N_0(z, t) - f_b N_1(z, t)) \\ &\quad \times \frac{I^+ + I^-}{h\nu} - \frac{N_1(z, t)}{\tau}, \\ N_t(z) &= N_0(z, t) + N_1(z, t), \end{aligned} \quad (1)$$

where  $I^+(z, t)$  is the intensity of the incident pump wave,  $I^-(z, t)$  is the intensity of the reflected pump wave,  $\sigma$  is the absorption cross section at pump wavelength,  $f_a$  is the Boltzmann coefficient of the ground

state population,  $f_b$  is the Boltzmann coefficient of the upper state population,  $N_0(z, t)$  is the number of atoms in the ground state,  $N_1(z, t)$  is the number of atoms in the excited state,  $h\nu$  is the photon energy,  $\tau$  is the excited state lifetime, and  $N_t(z)$  is the total number of atoms. Set of equations (1) was applied to analysis of a disk-shaped laser element with a thickness much smaller than its diameter. The element is assumed to be pumped by a parallel beam of thin monochromatic rays through the element's end. Pump radiation passes through the elements twice (incident and reflected waves), and the pump pulse is assumed to have a rectangular shape. Function  $N_t(z)$  represents the profile of concentration of the optical dopant along the direction of pump propagation. In real systems pumped by laser diode arrays, many thin rays propagate in different directions in different parts of the LE active

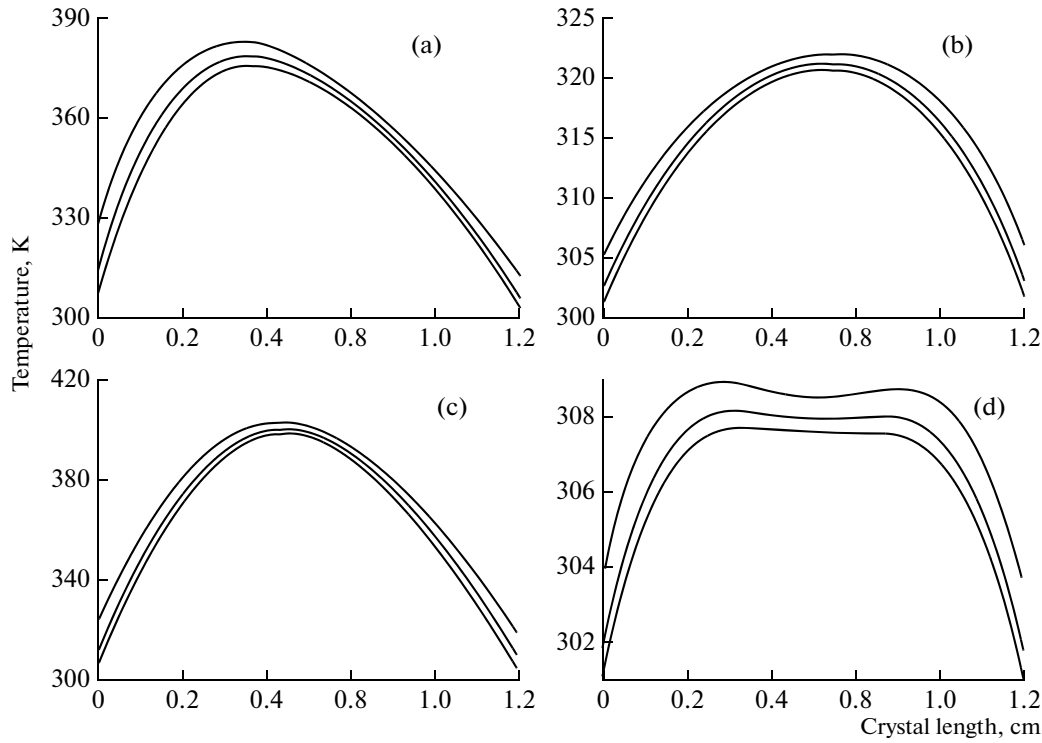


**Fig. 3.** Temperature field distribution in a crystal for different profiles of concentration: (a) constant, (b) exponential, (c) linearly increasing, and (d) parabolic.

medium. The total contribution of each source within an elementary interval of the laser diode array is equivalent to a system of thin rays propagating parallel to each other [2].

When analyzing a crystal containing two different kinds of optical centers, we used a model of a grid structure wherein the crystal was represented by a set of elementary plates of thickness  $dz$  containing only one kind of optical center. The result of propagation of incident and reflected waves is illustrated in Figs. 2d–2f for different distributions of concentration of optical centers along the  $z$  axis, which are presented in Figs. 2a–2c, respectively.

For mathematical modeling of thermal field distribution along the crystal coordinates, we analyzed set of differential equations (1) together with heat conductivity equation (2) with boundary conditions of the third kind for the one-dimensional case [1, 6]

$$\begin{aligned} \frac{d^2 T(z)}{dz^2} &= -\frac{q(z)}{\lambda}, \\ \left. \frac{dT(z)}{dz} \right|_{z=0} &= \frac{\alpha}{\lambda} (T(0) - T_f), \\ \left. \frac{dT(z)}{dz} \right|_{z=h} &= -\frac{\alpha}{\lambda} (T(h) - T_f), \end{aligned} \quad (2)$$

where  $T(z)$  is the crystal temperature at the corresponding point;  $q(z)$  is the total volume density of heat sources inside the crystal, which, according to (1), is equal to  $dI/dz$ , the derivative of pump intensity dissipated via nonradiative transitions;  $\lambda$  is the thermal conductivity (for YAG, it is equal to  $0.14 \text{ W cm}^{-1} \text{ K}^{-1}$ );  $\alpha$  is the heat exchange coefficient between the LE and surrounding medium (depends on the heat exchange geometry and the cooling substance), which was assumed to be 0.5, 0.6, and  $0.7 \text{ W/(cm}^2 \text{ K)}$  for an LE fabricated from YAG;  $T(0)$  and  $T(h)$  are temperatures of side surfaces of the LE at  $z = 0$  and  $z = h$ ; and  $T_f$  is the temperature of the surrounding medium, which was assumed to be 300 K.

The model of thermal field distribution is based on analysis of a disk LE. The side surface of the disk is thermally insulated, and the LE is conductively cooled through the edges. For numerical solution of set of equations (1)–(3), we used the finite difference method with a step size of  $4 \times 10^{-3} \text{ cm}$  [1, 6]. Since the characteristic times of thermal field propagation are small compared to the pulse duration, the heat conductivity equation is quasi-stationary. For analysis, we chose the constant, exponential, linearly increasing, and parabolic profiles of concentration illustrated in Fig. 1. Calculations were conducted for the case of pulsed pumping with pulse repetition rate  $f = 10 \text{ Hz}$ ,

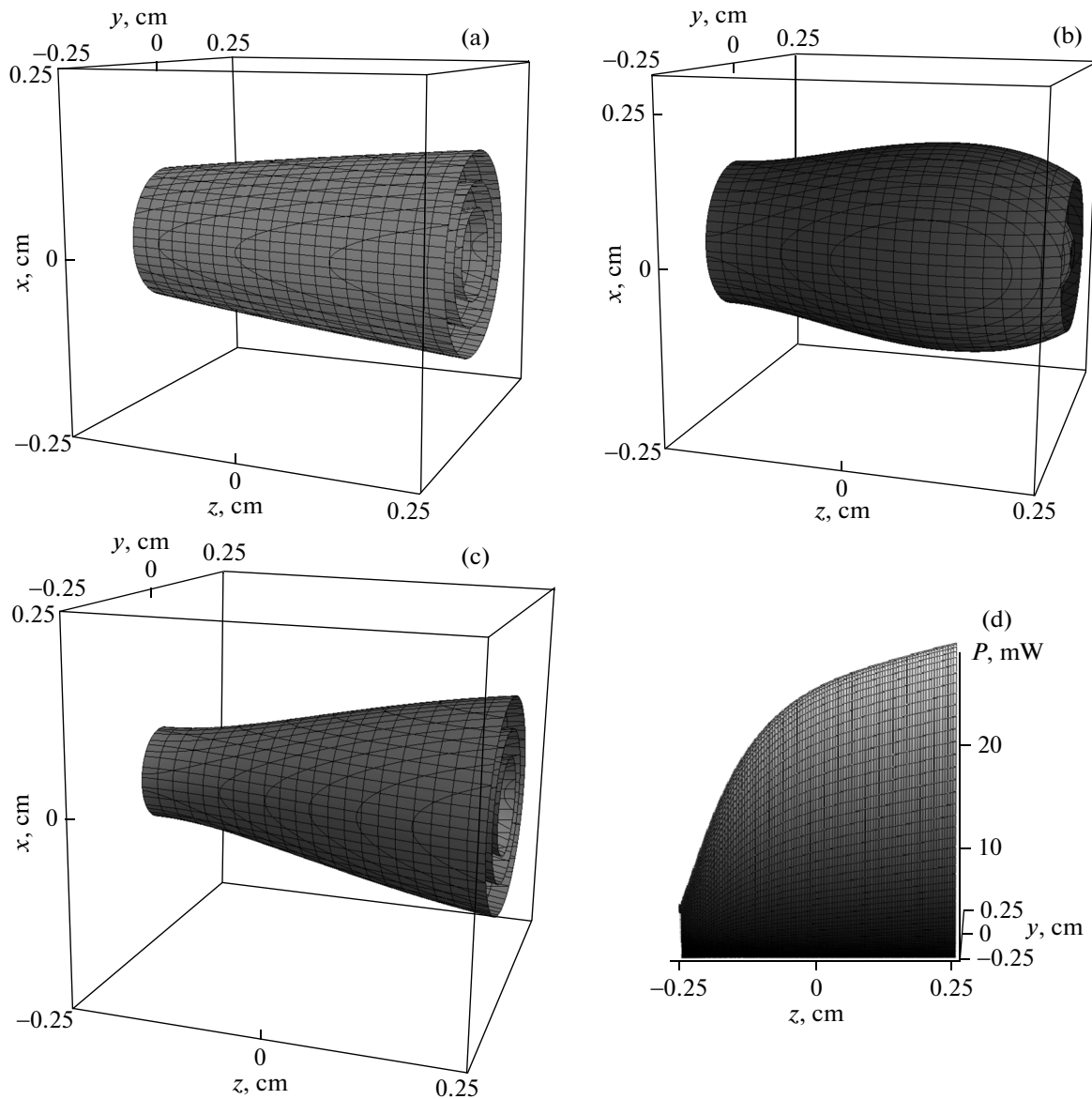


**Fig. 4.** Intensity distribution of a Gaussian mode in the cavity after one round trip (a–c) at (a) constant, (b) symmetric, and (c) asymmetric relative to crystal center distribution of optical centers (profiles of concentration are illustrated in Fig. 1, curves 1 and 2). Power distribution of optical radiation after double pass (d) in central section  $YZ$  ( $x = 0$ ) of a gradient YAG:Yb crystal (profile of  $\text{Yb}^{3+}$  concentration is shown in Fig. 1, curve 1),  $\lambda_p = 940$  nm.

pump pulse energy  $E_p = 0.3$  J, and pulse duration of  $300 \mu\text{s}$ . The model takes into consideration that the pump energy absorbed in some area of the crystal is divided between nonradiative transitions to metastable level (accompanied by heat release) and radiative transitions at the laser wavelength (a three-level scheme). It can be seen from the figures modeling thermal field distribution for a crystal with constant profile of doping impurity concentration (Fig. 3a) that the field distribution along the crystal represents a parabola with a maximum located at a certain distance from the crys-

tal ends. Three curves corresponding to each profile of concentration in Fig. 3 differ by values of heat exchange coefficient  $\alpha$  through the ends of a disk LE, which were 0.5, 0.6, and  $0.7 \text{ W}/(\text{cm}^2 \text{ K})$ , respectively. For an exponential profile of concentration (Fig. 1, curve 1), the distribution remains qualitatively the same (Fig. 3b).

The linearly increasing profile of concentration (Fig. 1, curve 3), which causes smoothing of the thermal lens upon pump propagation, creates a worse, compared to constant profile of concentration, ther-

Output radiation power (input signal 1 mW) in YAG crystals with different profiles of Yb<sup>3+</sup> concentration; pump power is 115 mW ( $\lambda_p = 940$  nm) and 120 mW ( $\lambda_p = 980$  nm)

Shape of gradient of Yb <sup>3+</sup> concentration	Radiation power in YAG:Yb crystals at $\lambda_{em} = 1050$ nm, mW	
	$\sigma_p = 3 \times 10^{-21}$ cm <sup>2</sup> $\lambda_p = 980$ nm	$\sigma_p = 1 \times 10^{-21}$ cm <sup>2</sup> $\lambda_p = 940$ nm
Uniformly doped	2.1 ( $z = 0.25$ cm)	9.4 ( $z = 0.25$ cm)
Symmetric parabola	1.0 ( $z = 0.25$ cm)	1.0 ( $z = 0.25$ cm)
	1.9 ( $z = 0.08$ cm)	7.3 ( $z = 0.08$ cm)
Asymmetric parabola	3.1 ( $z = 0.25$ cm)	28.9 ( $z = 0.25$ cm)

mal field distribution along the crystal length. Such a pattern is created because most of the radiation is absorbed in the crystal center, where the possibility of heat dissipation is limited (Fig. 3c).

For a parabolic profile of concentration (Fig. 1, curve 2), the temperature gradient is strongly reduced (Fig. 3d). About 80% of the LE length has, on average, the same temperature, and the magnitude of temperature nonlinearity  $\Delta T$  does not exceed 8 K, provided that ambient temperature is 300 K. To determine the steady-state configuration of the lower Gaussian mode, we studied laser elements with different profiles of concentration (Fig. 1, curves 1 and 2). Figure 4 illustrates a Gaussian mode for an LE with different gradients of concentration, where the pump intensity distribution varies in accordance with the expression [7]

$$U = G \frac{b}{\sqrt{z^2 + b^2}} \exp \left[ -\frac{kbr^2}{2(z^2 + b^2)} \right] + i \left( \frac{kr^2 z}{2(z^2 + b^2)} - \arctan \left( \frac{z}{b} \right) + kz + \varphi \right), \quad (3)$$

Here,  $b = ka^2$  is the confocal parameter;  $a$  is the waist radius, which is equal to 0.125 cm (specified as an external parameter) in the case under consideration;  $k$  is the wavenumber;  $\varphi$  is the initial phase;  $G$  is the amplitude coefficient including the dependence on gradient of concentration of optical centers, which is given by

$$G = \sqrt{\exp(\sigma_{em} F(z) m h z)}, \quad (4)$$

where  $\sigma_{em}$  is the emission cross section;  $\sigma_{em} (\lambda_{em} = 1050 \text{ nm}) = 5 \times 10^{-21} \text{ cm}^2$  for YAG:Yb; and  $F(z)$  is the gradient of dopant concentration normalized to its peak value in atomic percent ( $m = 16.5$  at %) and concentration corresponding to 1 at % ( $h = 1.36 \times 10^{20} \text{ cm}^{-3}$ ). To find the optical radiation power, we cal-

culated the square of the real part of Gaussian beam intensity (3)

$$U = \left\{ \text{Re} \left[ G \frac{b}{\sqrt{z^2 + b^2}} \exp \left( -\frac{kbr^2}{2(z^2 + b^2)} \right) \right] \right\}^2. \quad (5)$$

Thus, variation in the intensity of a Gaussian mode along the crystal in the cavity per round trip (for different profiles of concentration) has the form presented in Figs. 4a–4c. After several cavity roundtrips, the intensity distribution becomes more uniform. The profile of this distribution after two passes of the wave through the active medium for central YZ ( $x = 0$ ) plane section of the gradient crystal is illustrated in Fig. 5.

The calculated values of radiation power obtained in the regime of small signal gain after propagation through YAG:Yb crystals exhibiting a gradient of dopant concentration and crystals with uniform dopant distribution calculated at a wavelength of  $\lambda_{em} = 1050$  nm for the same pump power are presented in the table. The values of power were calculated for coordinates of the output face of the crystals ( $z = 0.25$  cm); the crystal center is located at  $z = 0$ . The table also shows the peak values of the output power achieved at  $z = 0.08$  cm.

The results of calculations show that the proposed method of crystal growth allows not only controlling the composition of monocrystals, but also forming laser media, which yield a larger fraction of absorbed pump power under longitudinal pumping compared to uniformly doped optical media. This fact indicates a higher efficiency of optical pumping of laser crystals in the case of a specially shaped gradient of the optical dopant concentration in the laser element.

## ACKNOWLEDGMENTS

This work was supported by the Russian Ministry of Education and Science through the federal targeted program “Scientific and Pedagogical Personnel of

Innovative Russia (2009–2013)” and the program of development of students' organizations of Kuban State University.

#### REFERENCES

1. T. N. Alpat'ev, V. A. Smirnov, and I. A. Shcherbakov, *Kvantovaya Elektron.* No. 39, 1033 (2009).
2. T. Y. Fan, *IEEE J. Quantum Electron.* **28** (12), 2692 (1992).
3. N. V. Kravtsov, *Kvantovaya Elektron.* No. 31, 661 (2001).
4. V. V. Galutskiy, M. I. Vatlina, and E. V. Stroganova, *J. Crystal Growth*, No. 311, 1190 (2009).
5. V. V. Galutskii, N. A. Yakovenko, and E. V. Stroganova, *Opt. Spectrosc.* **110** (3), 401 (2011).
6. A. N. Alpat'ev, V. A. Smirnov, and I. A. Shcherbakov, *Kvantovaya Elektron.* No. 1, 35 (2010).
7. V. P. Bykov and O. O. Silichev, *Laser Resonators* (Fizmatlit, Moscow, 2004; Cambridge International Science Publishing, 2009).